Available online at www.sciencedirect.com
SCIENCE DIRECT®
Journal of Catalysis 222 (2004) 357–367
JOURNAL OF CATALYSIS
www.elsevier.com/locate/jcat

Characterization and reactivity in CO oxidation of gold nanoparticles supported on TiO_2 prepared by deposition-precipitation with NaOH and urea

Rodolfo Zanella,[a] Suzanne Giorgio,[b] Chae-Ho Shin,[c] Claude R. Henry,[b] and Catherine Louis [a,*]

[a] *Laboratoire de Réactivité de Surface, UMR 7609 CNRS Université Pierre et Marie Curie, 4 place Jussieu, 75252 Paris cedex 05, France*
[b] *CRMC2 CNRS, Campus de Luminy, case 913, associated to the Universities of Aix-Marseille II and III, 13288 Marseille cedex, France*
[c] *Department of Chemical Engineering, Chungbuk National University Cheongju, Chungbuk 361-763, South Korea*

Received 11 August 2003; revised 3 November 2003; accepted 5 November 2003

Abstract

Au/TiO_2 catalysts were prepared by deposition-precipitation with NaOH (DP NaOH) (∼ 3 wt% Au) and urea (DP Urea) (∼ 8 wt% Au), and calcined at various temperatures between 100 and 400 °C. They were characterized by UV-visible absorption, XANES, EXAFS, and TEM. Their activity was tested in the reaction of CO oxidation at 5 °C. After preparation, the gold species are in the oxidic state III. They begin to transform into metallic gold under air at ∼ 100 °C for DP NaOH and ∼ 150 °C for DP Urea. At 200 °C, all the gold is metallic for the two preparation methods. The particle size increases from 1.5 to 3.5 nm with the calcination temperature. The catalytic activity for CO oxidation increases with the percentage of metallic gold, and it is maximum after calcination at 200 °C for both types of samples. The activities (per mole of Au) and TOF are the same for the two types of catalysts. After higher calcination temperatures, the catalytic activity drops. The decrease of activity is mainly due to a change of particle shape with the calcination temperature rather than to the increase of the particle size. At a pretreatment temperature of 200 °C, the particles present small facets with rounded parts, and their outer surface contains a large proportion of low-coordinated sites (steps and corners) while at higher temperatures of pretreatment, they are truncated octahedra with smooth facets.

Keywords: Gold; Catalyst; Metal nanoparticle; Titania; Catalyst preparation; Deposition-precipitation; UV-visible; EXAFS; TEM; CO oxidation

1. Introduction

Until the end of the 1980s, only very limited attention has been paid to catalysis with gold metal because of its electronic configuration of noble metal, which is usually accompanied by very low activities [1]. This situation has been changed in recent years with the discovery of the catalytic activity of gold nanoparticles [2]. Gold catalysts have recently attracted growing interest due to their potential for many reactions of both industrial and environmental importance. The most remarkable catalytic properties of supported gold have been first obtained for the reaction of CO oxidation at subambient temperature by Haruta et al. in 1987 [3].

Gold can also be active in various other reactions, selective hydrogenation, water–gas shift, reduction of NO with hydrocarbons, epoxidation of propylene, CO and CO_2 hydrogenation, and in reactions involving halogens [4,5].

The most studied catalyst for CO oxidation is gold supported on TiO_2 because it is one of the most active catalysts for this reaction at low temperature. The optimum gold particle size in these catalysts was found to be 2–3 nm [6,7]. Such particle sizes can be achieved owing to suitable preparation methods and careful control of the conditions of preparation.

Up to now, for the preparation of Au/TiO_2 catalysts, the best method has been the deposition-precipitation with NaOH [8] because it allows the size of the gold particles to be adjusted by controlling the pH of the preparation and the calcination temperature. However, we have recently developed a new preparation method of Au/TiO_2 catalysts using deposition-precipitation with urea [9]. It gives the same gold particle sizes as those obtained by Haruta et al. with the method of deposition-precipitation with NaOH [8,10], i.e., 2–3 nm. The main advantage of this new method over that

* Corresponding author.
E-mail address: louisc@ccr.jussieu.fr (C. Louis).

0021-9517/$ – see front matter
doi:10.1016/j.jcat.2003.11.005

of deposition-precipitation with NaOH is that all the gold from the solution is deposited on TiO_2, so higher gold loading can be reached, and the gold loading of the catalysts can be easily controlled.

In the literature, there is no agreement on the optimal calcination temperature for the Au/TiO_2 catalysts for the CO oxidation reaction. Some papers report that highly active gold catalysts must be calcined at temperatures above 300 °C [2,11] while others claim that lower calcination temperatures produce catalysts with higher activities [12,13]. According to Haruta et al. [14], the calcination at 300 °C (in air) is necessary to form metallic gold particles, which strongly interact with the metal oxide support. Boccuzzi et al. [15] studied a Au/TiO_2 (1 wt%) catalyst calcined at three different temperatures, 200, 300, 600 °C, and they found the best performance on CO oxidation for the catalysts calcined at 200 and 300 °C. The higher catalytic activity at these temperatures was related to the higher concentration of step sites over the Au surfaces and to a larger concentration of step sites at the borderline with the support. Daté et al. [16] suggested that calcination at temperatures above 300 °C is necessary to reduce oxidic gold species in metallic gold, although the catalytic activity of the catalysts calcined at 200 °C increased after exposure to ambient conditions for a few days and exceeded those from the catalyst calcined at 300 °C.

Many authors [5,7,12,17] suggest that the activity of gold supported on TiO_2 strongly depends on the size of the gold particles with a maximum of activity usually observed for a particle size of about 3 nm. Boccuzzi et al. [15] observed that the rate of the CO oxidation reaction markedly increases with a decrease in the diameter of the Au particles. It was claimed [18] that the effect of the oxidation state of gold is at least as important as that of the particle size of the metallic gold. However, the state of the gold in active catalysts is unclear. Hoflund and co-workers claimed that part of the gold supported in α-Fe_2O_3 and Co_3O_4 is nonmetallic, and that it may be responsible for the low-temperature activity [19,20]. Park and Lee [18] concluded from XPS investigations that oxidic gold is the active species in catalysts of gold supported on TiO_2, Al_2O_3, and Fe_2O_3. Visco et al. [21] found much larger catalytic activity in uncalcined samples than in calcined ones and proposed that oxidized gold species are the most active sites for low-temperature CO oxidation for Au/Fe_2O_3 catalysts [22]. Minicò et al. [23] found a correlation between the occurrence of an IR band, assigned to the adsorption of CO on Au^+, and the catalytic activity of coprecipitated Au/Fe_2O_3 catalysts. Some other papers report partially oxidized forms of gold in Au/Fe_2O_3 [14], Au/Co_3O_4 [24], Au/Al_2O_3 catalysts [25], and Au/MgO [26].

In a study combining ab initio calculations and experiments, Sanchez et al. [27] found that 8 atom gold clusters deposited on defective MgO surfaces are active in CO oxidation while they are inactive if they are deposited on a perfect surface. This difference of activity is explained by a charge transfer from an F center (oxygen vacancy) on the MgO surface toward the gold clusters where it is attached. This result is in agreement with results on unsupported gold clusters (below 20 atoms) showing that anionic clusters are reactive with oxygen, while cationic ones are not [28,29]; anionic clusters can even produce CO_2 by successive exposures to CO and O_2 [30].

In contrast, many other authors suggest that metallic gold is the active species in Au/TiO_2, $Au/Ti(OH)_3$, or Au/ZrO_2 [5,31–34].

In this work, we have prepared Au/TiO_2 catalysts by two methods, deposition-precipitation with NaOH (DP NaOH), i.e., the Haruta method [8], and deposition-precipitation with urea (DP Urea), developed by us [9]. The goal of this study was threefold: (i) to compare the catalytic behavior of these two types of catalysts in the reaction of CO oxidation; (ii) to determine the calcination temperature for which these catalysts are the most active for this reaction; (iii) to determine the oxidation state of the gold species active in this reaction.

2. Experimental

2.1. Au/TiO_2 preparations

Titania Degussa P25 was used as support (45 $m^2\,g^{-1}$, nonporous, 70% anatase and 30% rutile, purity > 99.5%) and solid $HAuCl_4 \cdot 3H_2O$ (Acros) as gold precursor. Before preparation, TiO_2 was previously dried in air at 100 °C for at least 24 h. The preparations were performed in the absence of light, which is known to decompose and reduce gold precursors.

For the Au/TiO_2 preparations by deposition-precipitation with NaOH (DP NaOH), 100 mL of an aqueous solution of $HAuCl_4$ (4.2×10^{-3} M) was heated to 80 °C. The pH was adjusted to 7 by dropwise addition of NaOH 1 M, then 1 g of TiO_2 was dispersed in the solution and the pH was readjusted to 7 with NaOH. The suspension thermostated at 80 °C was vigorously stirred for 2 h.

For the Au/TiO_2 preparations by deposition-precipitation with urea (DP Urea), 1 g of TiO_2 was added to 100 mL of an aqueous solution containing $HAuCl_4$ (4.2×10^{-3} M) and urea (0.42 M). The initial pH was ~ 2. The suspension thermostated at 80 °C was vigorously stirred for 16 h. Urea decomposition leads to a gradual rise in pH from 2 to 7.

In both DP NaOH and DP Urea preparations, the amount of gold in solution corresponds to a maximum gold loading of 8 wt% on TiO_2.

The solids were gathered by centrifugation (12,000 rpm for 10 min), washed in 100 mL of distilled water under stirring for 10 min at 50 °C, and then centrifuged. The operation was repeated four times. The solids were dried under vacuum at room temperature for 16 h or at 100 °C for 2 h or in air at room temperature for 48 h. The dried samples were stored away from light and under vacuum in a desiccator.

Before characterization, the dried samples were calcined at various temperatures, between 150 and 400 °C, under a

flow of industrial air (100 mL min^{-1}, Air Liquide) with a heating rate of 2 °C min^{-1} and then maintained 4 h at the chosen temperature. Sample transfers were performed in air to various spectrometers for characterization as fast as possible.

2.2. Characterization techniques

Chemical analysis of Au was performed on calcined samples by inductively coupled plasma atom emission spectroscopy at the CNRS Center of Chemical Analysis (Vernaison, France). The Au weight loading of the samples is expressed in grams of Au per gram of sample calcined at 1000 °C: wt% Au $= [m_{\mathrm{Au}}/(m_{\mathrm{Au}} + m_{\mathrm{TiO_2}})] \times 100$.

The gold loading is 3.1 wt% for the DP NaOH catalyst and 7.6 wt% for the DP Urea catalyst, and Cl loading is 100 and 300 ppm, respectively.

The UV-visible spectra (200–2500 nm) of the Au/TiO_2 samples were carried out on a Cary 5E spectrophotometer equipped with a Cary4/5 diffuse reflection sphere. The baseline was recorded using a poly(tetrafluoroethylene) reference.

The calcined Au/TiO_2 samples were examined by transmission electron microscopy (TEM). The morphology, structure, and chemical analysis were determined either in low resolution and EDS with a JEOL 2000 FX microscope or in high resolution with a JEOL 3010 microscope. For the observation, the catalysts were dispersed on a copper grid precovered with a carbon film. For a better stability, especially in the high-resolution mode, the samples were covered by a thin carbon layer (less than 5 nm thick). The distances between the lattice planes in the gold particles, imaged by HRTEM, were measured by numerical analysis using the TiO_2 lattice for internal calibration. The histograms of the metal particle sizes were established from the measurement of 500 to 1000 particles. The size limit for the detection of gold particles on TiO_2 was about 1 nm. The average particle diameter d_s was calculated using the following formula: $d_s = \sum n_i d_i^3 / \sum n_i d_i^2$ where n_i is the number of particles of diameter d_i.

XAS (X-ray absorption spectroscopy) measurements of the Au/TiO_2 samples were performed at the Au L_{III} edge at the XAS 13 beam line of the DCI storage ring of LURE synchrotron radiation facility (Orsay, France). The samples were diluted with cellulose and pressed as a pellet. The XANES spectra (X-ray absorption near-edge structure) and EXAFS signals (extended X-ray absorption fine structure) were recorded at room temperature, in the transmission mode, using two argon-filled ionization chambers and a channel-cut Si(111) monochromator. For each sample, the XANES spectra were scanned two times with 0.5 eV steps from 11,870 to 12,020 eV, and the EXAFS signals were scanned five times with 2 eV steps from 11,750 to 12,750 eV. The energy was calibrated using a Au metal foil. The XAS spectra of references, gold foil, $Au(OH)_3$, and $HAuCl_4$ were also recorded.

After background correction, the XANES spectra were normalized in the middle of the first EXAFS oscillation. The EXAFS analyses were done in the framework of single scattering treatments with the package of programs EXAFS pour le Mac [35] since data analyses were limited to the first shell only. The $k\chi(k)$ functions were extracted from the data following the procedure proposed by Lengeler and Eisenberger [36] using a linear preedge background and a cubic spline atomic absorption background. The Fourier transforms (FT) were calculated on $w(k)k\chi(k)$, where $w(k)$ is a Kaiser–Bessel window with a smoothness parameter equal to 3. The k limits are 3 and 14 Å^{-1}. It may be noted that the FTs are presented without phase correction in the figures. Single scattering fits of experimental curves were performed with the Round Midnight program [35], which uses the minimization capabilities of the Minuit code [37]. The constant of the mean free path Γ_i was extracted from references (metallic gold foil) and $Au(OH)_3$, $\Gamma_{\mathrm{Au–Au}} = 0.82$ and $\Gamma_{\mathrm{Au–O}} = 0.4$. The inelastic reduction factor S_0^2, and the functions $|f_i(k, R_i)|$ (amplitude) and $|\phi_i(k, R_i)|$ (phase shift) were calculated from the structures of metallic gold, and Au_2O_3 using the FEFF 7.0 code [38,39].

Catalytic measurements of CO oxidation were carried out in a fixed-bed reactor using $\sim$ 25 mg of DP NaOH catalysts and $\sim$ 15 mg of DP Urea catalysts, but accurately weighed for each sample. The catalysts previously dried at 100 °C were calcined as described above at the desired temperature for 4 h. After calcination, the reactor was cooled to 5 °C under air, which was replaced by a gas mixture consisting of 1% vol CO and 4% O_2 balanced with N_2 to 1 atm (99.3 mL min^{-1}). CO was analyzed at the outlet of the reactor with an IR detector (COSMA Beryl 100).

The turnover frequency (TOF), number of molecules of CO converted per surface atom of gold particles and per second, was calculated for the two series of catalysts with the assumption that gold particles were cubo-octahedra. This hypothesis is supported by HRTEM observation (see next section). The dispersion D was calculated by the formula $D = N_s/N_t$, where N_s represents the number of surface atoms and N_t the total number atoms in the particle.

3. Results

3.1. Characterization by UV-visible spectroscopy

Fig. 1A displays the UV-visible spectra of DP Urea series, the sample dried at RT and at 100 °C under vacuum, and those calcined at 150, 200, 300, and 400 °C in air. The spectra of the samples dried at RT under vacuum and calcined at 100 °C only show the absorption of TiO_2 below 400 nm. The spectra of the samples calcined at higher temperature ($T \geqslant 150$ °C) exhibit another band around 550 nm, the intensity of which increases with the calcination temperature. This band is characteristic for the plasmon resonance of metallic gold particles. In metal nanoparticles of Au^0, Cu^0,

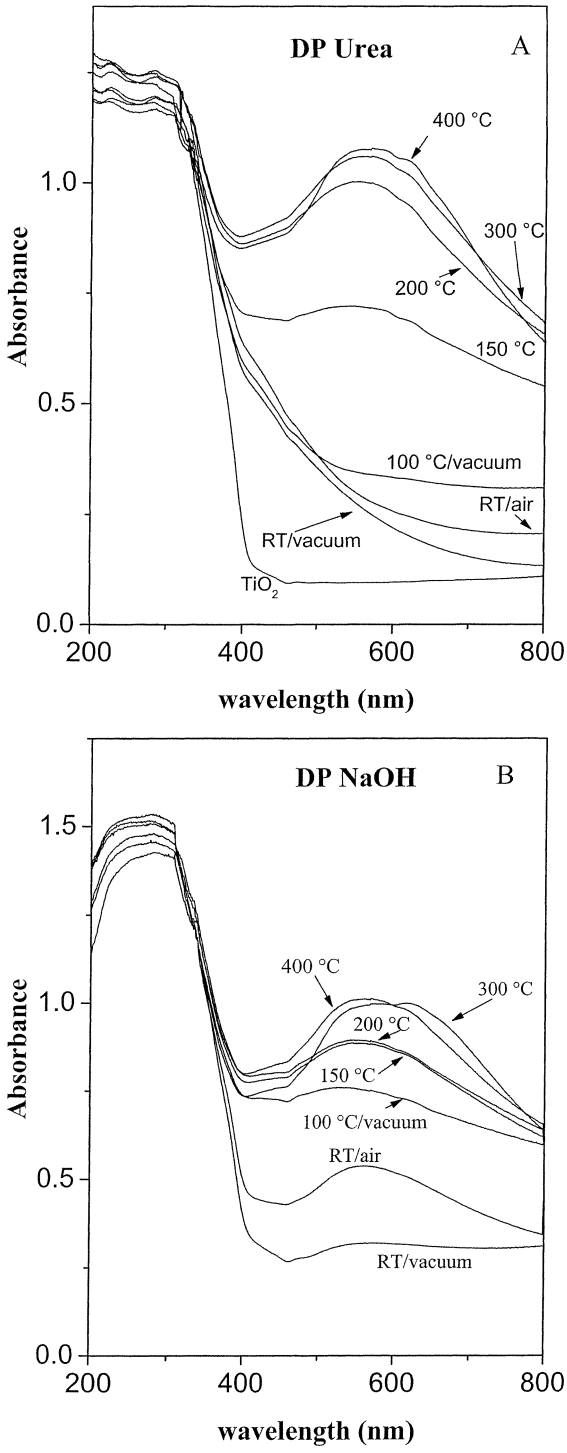

Fig. 1. UV-visible spectra of pure TiO_2 and the DP Urea (A) and DP NaOH samples (B) as a function of the temperatures of drying (RT and 100 °C) and calcination under air (150 to 400 °C).

and Ag^0, the plasmon absorption arises from the collective oscillations of the free conduction band electrons that are induced by the incident electromagnetic radiation. Such resonances are seen when the wavelength of the incident light far exceeds the particle diameter. In DP Urea samples, the plasmon band begins to appear after calcination at 150 °C (Fig. 1A). It is clearly visible after calcination at 200 °C, and it evolves almost no longer at higher temperature, suggesting that the gold particles are fully metallic.

Fig. 1B presents the UV-visible spectra of the DP NaOH series, the sample dried at RT and 100 °C under vacuum, and those calcined at 150, 200, 300, and 400 °C in air. The evolution of the plasmon band with temperature is different from that observed for the DP Urea series. A weak band is visible in the spectrum of DP NaOH sample after drying at RT under vacuum that increases after drying at RT under ambient air. After drying at 100 °C under vacuum, the plasmon band begins to appear, and it is clearly visible after calcination at 150 °C. Thus, we can conclude that there is a difference in reducibility of gold in DP NaOH and DP Urea samples. The DP NaOH sample is already partially reduced at 100 °C whereas the DP Urea one is not reduced at this temperature. In addition, when DP NaOH samples were dried at RT under vacuum, there was no well-developed plasmon band visible in the UV-visible spectrum, but only a shoulder. However, when this sample was dried in air at RT, a plasmon band was clearly identified. In DP Urea samples, this behavior was not observed, after drying a RT in air.

The presence of a plasmon band at $T \geqslant 150$ °C in DP Urea and at $T \geqslant 100$ °C in DP NaOH shown in Fig. 1 indicates that (i) after preparation, and therefore during preparation, gold is not reduced, and is probably in the oxidation state of the precursor, i.e., Au^{III}; (ii) the exposition of the DP NaOH catalyst to air, even at RT, starts to induce the reduction of gold; (iii) the reduction of gold increases with temperature.

Noteworthy is the change of color of the samples during preparation/activation, which is also an indication of the oxidation state of gold. In DP NaOH samples, the white color of the wet sample changed to gray after drying under vacuum at RT. It changed to gray-purple after calcination at 100 °C and to purple after calcination at temperatures above 150 °C. Purple color is characteristic of metallic small gold particles [40]. In the DP Urea samples, the initial yellow-orange color of the wet sample is almost unchanged after drying under vacuum at RT or at 100 °C or after calcination in air at 100 °C. It begins to turn to purple after calcination at $T \geqslant 150$ °C. The difference of color between the two samples dried at RT indicates that the nature of the gold species deposited during DP Urea is different from that deposited during DP NaOH. This has been recently confirmed (unpublished results).

In addition to the different reducibilities of the two types of samples, there are two other main differences between the spectra of DP Urea and DP NaOH samples (Fig. 1):

– the different intensities of the plasmon band on the fully reduced samples, which are due to the different gold loadings (8 and 3 wt%);

– the absorption at 400–600 nm in the DP Urea samples dried at RT or 100 °C. In our opinion, it is due to the absorption of the orange gold phase which is deposited during DP Urea.

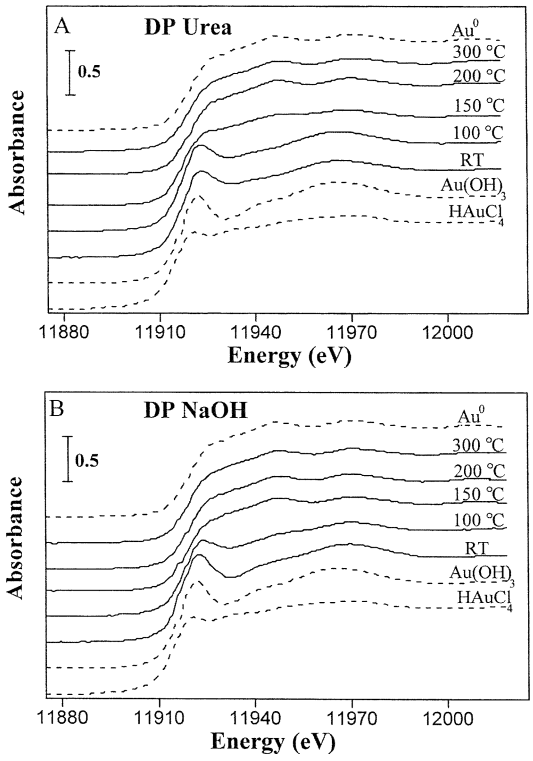

Fig. 2. Normalized XANES spectra of references ($HAuCl_4$, $Au(OH)_3$, Au^0), the DP Urea (A) and DP NaOH samples (B), as a function of the temperatures of drying (RT and 100 °C under vacuum) and calcination under air (150 to 400 °C).

3.2. XAS spectroscopy

Fig. 2 presents the normalized XANES spectra of the DP Urea and DP NaOH samples as a function of the temperature of drying/calcination. As references, the spectra of Au^{III} ($Au(OH)_3$ and $HAuCl_4$) and Au^0 (gold foil) were recorded. Compared to the XANES spectra of the references, those of the DP Urea samples treated at room temperature and 100 °C (Fig. 2A) are more like that of $Au(OH)_3$ spectrum than to that of $HAuCl_4$ spectrum. The spectra of the DP Urea samples treated at 200 and 300 °C are very similar to the spectrum of metallic gold, whereas the sample treated at 150 °C is intermediate. In the case of DP NaOH samples, only the spectrum of the sample dried at RT under vacuum (Fig. 2B) is similar to the spectrum of $Au(OH)_3$; the spectrum of the sample calcined at 100 °C is intermediate between the spectra of the two references, and at a calcination temperature higher than 150 °C, the spectra are the same as the spectrum of the gold foil.

To determine the percentage of Au^0 in the "intermediate" samples, a series of linear combinations between a reference containing Au^{III} and the reference containing Au^0 was performed. The results of these combinations were compared to the experimental XANES spectra. For DP NaOH samples, the spectra of Au^0 and $Au(OH)_3$ sample were taken as reference to perform the linear combinations. For DP Urea samples, the linear combinations were performed using the spectrum of DP Urea dried at RT as reference for Au^{III} because the nature of the gold species deposited during DP Urea is different from that deposited during DP NaOH as noted in the former paragraph. We also checked that the fit with the spectrum of $Au(OH)_3$ was not as good as for DP NaOH. The choice of the spectrum of DP Urea dried at RT as reference was justified by the UV-visible absorption results in Fig. 1A, which show that the DP Urea sample dried under vacuum at room temperature does not present the plasmon band; so, there is no metallic gold in this sample (this approximation will be also justified by the EXAFS results). Hence, our calculations (see Table 1) show that in the DP Urea sample calcined at 150 °C, 70% of gold is metallic. By the same procedure, we found that the metallic gold begins to form at 100 °C (40%) in DP NaOH samples. For the sample DP NaOH calcined at 150 °C, it is not possible to determine if all gold is in the metallic state or if a little quantity of Au ($\leqslant 10\%$) is in the oxidized state; this is beyond the precision of the technique.

Table 1
Percentage of metallic gold determined from XANES, in the DP NaOH and DP Urea catalysts as a function of drying/calcination temperature

Pretreatment temperature (°C)	Au^0 in DP DP NaOH (%)	Au^0 in DP DP Urea (%)
RT	0	0
100	40	0
150	90–100	70
300	100	100

It is important to note that in both cases, the samples dried at room temperature contains only Au^{III} according to XANES and that in DP Urea sample calcined at 100 °C, there is no metallic gold.

Fig. 3 shows the modulus of the Fourier transform of the EXAFS signals (i.e., the pseudo RDF), without phase correction, for the DP Urea and DP NaOH samples. The FTs of DP Urea dried at RT and calcined at 100 °C (Fig. 3A) and the DP NaOH dried at RT (Fig. 3B) are almost identical to that of $Au(OH)_3$. There is a first very intense peak at $R = 1.65$ Å. The DP Urea sample calcined at 150 °C and the DP NaOH samples calcined at 100 and 150 °C show a tiny peak at 1.65 Å, which could correspond to $Au(OH)_3$, and a more intense peak at 2.72 Å that corresponds to metallic gold. The moduli of the FTs of the DP Urea and DP NaOH samples calcined at 200 and 300 °C are almost identical to that of metallic gold.

Table 2 summarizes the results of the best fits of the EXAFS signals for first neighbors in the DP Urea series and DP NaOH series. It shows in the DP Urea series that for the samples dried under vacuum at room temperature and calcined at 100 °C, the only backscatterer is O at a distance of 2.0 Å, and there is no Au as first neighbor. This indicates that all gold is oxidized, in agreement with XANES results. On the contrary, at 150 °C, there are two backscatterers, O and Au, so the sample contains a mixture of Au^{III}

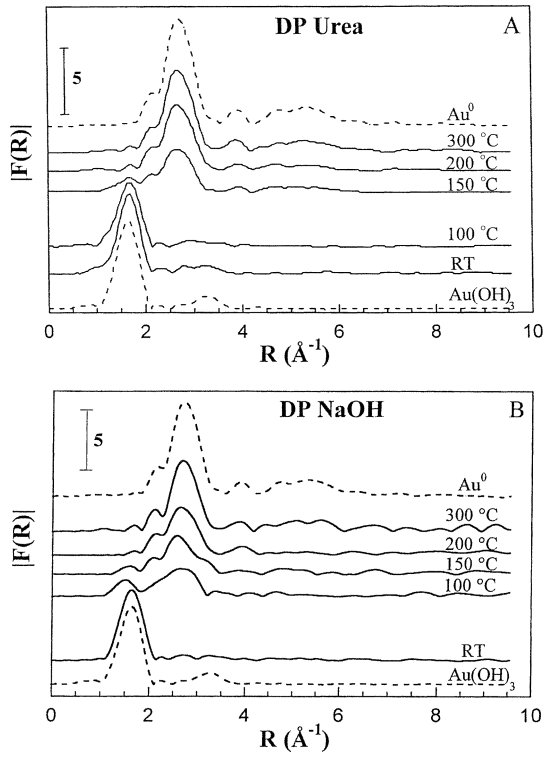

Fig. 3. Modulus of the Fourier transforms of the EXAFS signals of references ($Au(OH)_3$, Au^0), the DP Urea (A) and DP NaOH samples (B), as a function of the temperatures of drying (RT and 100 °C under vacuum) and calcination under air (150 to 400 °C).

and Au^0. A calculation by linear combination of the EXAFS spectra of gold foil and of DP Urea dried at RT was performed and compared to the spectrum of DP Urea calcined at 150 °C. The result shows that 70–80% of the backscatterers is Au and the remaining part is O. This result is consistent with XANES (75% of gold is in the metallic state) (see Table 1). In DP Urea calcined at 300 °C, the only backscatterer is Au, confirming that the gold particles are completely reduced.

For the DP NaOH series, according to EXAFS results for the first neighbors (Table 2), gold species are mainly in the Au–O-bonding environment when dried at 25 °C. After calcination at 100 and 150 °C, the gold species are in the Au–O- and Au–Au-bonding environment. This is in agreement with the XANES results obtained after calcination at 100 °C where a mixture of Au^{III} and Au^0 was found. For the sample calcined at 150 °C, the EXAFS results show a weak percentage of a Au–O-bonding environment, although the presence of Au^{III} was not detected by XANES. The sample is therefore not fully reduced, but the amount of Au^{III} is probably smaller or equal to 10% (accuracy limit of the XANES quantification). For higher calcination temperatures, 200 and 300 °C, the gold species are in an Au–Au-bonding environment, in agreement with XANES results.

In DP Urea and DP NaOH calcined at 200 and 300 °C, all the gold is in the metallic state with a coordination number smaller than in the gold foil. This is consistent with the presence of small gold particles. The results presented in Table 2 support the XANES results of the DP Urea samples, that only Au^{III} is present in the sample dried at RT. All the results obtained by XANES and by EXAFS are coherent and allow the conclusion that gold begins to reduce at ~ 100 °C in the DP NaOH sample and at ~ 150 °C in the DP Urea samples.

Table 2
Best parameters for the fit of the EXAFS signals of Au references and Au/TiO_2 samples for DP Urea and DP NaOH series

Samples	Back-scatterers	N	σ (Å)	R (Å)	ΔE_0 (eV)	ρ (%)
Gold foil	Au	12	0.089	2.85	3.4	0.9
$Au(OH)_3$	O	4.0	0.059	1.98	7.1	0.4
DP Urea RT	O	4.0	0.060	2.00	8.0	2.1
DP Urea (100 °C)	O	3.8	0.065	2.00	8.9	1.0
DP Urea (150 °C)	O	1.0	0.070	2.00	8.0	1.0
	Au	8.1	0.101	2.83	1.1	
DP Urea (200 °C)	Au	10.0	0.094	2.83	4.1	1.5
DP Urea (300 °C)	Au	11.0	0.091	2.84	3.7	1.5
DP NaOH (RT)	O	4.1	0.041	1.97	6.0	0.7
DP NaOH (100 °C)	O	0.9	0.080	1.95	5.1	5.0
	Au	7.1	0.106	2.80	1.3	
DP NaOH (150 °C)	O	0.3	0.060	2.00	1.1	3.3
	Au	8.1	0.102	2.81	4.3	
DP NaOH (200 °C)	Au	10.0	0.100	2.83	4.2	0.9
DP NaOH (300 °C)	Au	10.7	0.093	2.84	2.9	1.7

N, number of neighbors; σ, Debye–Waller factor; R, distance between Au and a backscatterer; ΔE_0 (eV), energy shift; ρ, agreement factors, $\Gamma_{\text{Au–Au}} = 0.82$, and $\Gamma_{\text{Au–O}} = 0.4$.

3.3. HRTEM observation

The morphology, structure, and orientation of the gold particles on the TiO_2 support, after different pretreatment temperatures, have been determined by HRTEM. Fig. 4A shows a 2-nm gold particle from a DP Urea sample pretreated at 200 °C under H_2 (the same type of images is obtained after pretreatment at 200 °C under air, but the image analysis has not yet been done). The interface is not completely flat. Among all the observed particles, no preferential orientation could be observed. The particles are single crystals and present some tiny facets and rounded parts. They are stable under the electron beam. Fig. 4B corresponds to particles from the same initial preparation after pretreatment at 500 °C under H_2. The particles are now perfectly faceted and present the unique shape of a truncated octahedron exposing (111) and (100) facets. They are stable under electron beam irradiation, and their interface is flat. It is noteworthy that after calcination under air between 300 and 400 °C, the same particle shape is observed. Occasionally, some particles are observed by HRTEM in epitaxy on the TiO_2 support. Fig. 4B shows a gold particle in epitaxy on the TiO_2 substrate. The (111) plane of gold is parallel to the (110) plane of the rutile (the titania support is composed of 30% of rutile). By numerical analysis,

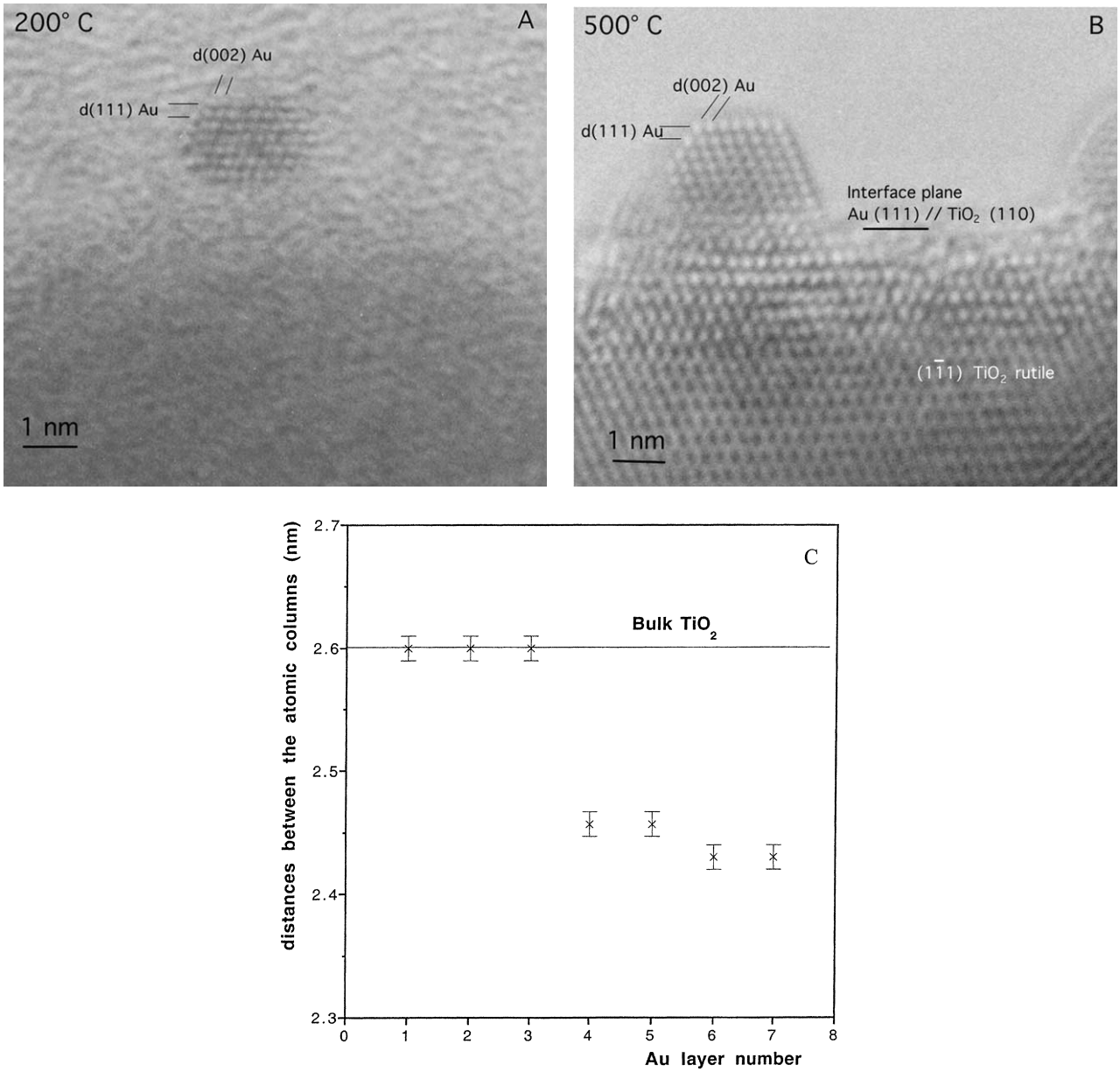

Fig. 4. HRTEM images of gold particles in the profile view in the DP Urea sample reduced under H_2 (A) at 200 °C, (B) at 500 °C (the view axis, perpendicular to the image, is in the [110] direction); (C) average lattice distance in the successive layers starting from the interface.

the intensity profiles in the (111) lattice planes, parallel to the interface, have been recorded from the interface until the top of the particle. As seen on Fig. 4C, the gold particle is accommodated to the lattice of the support in the three first layers from the interface, that means a 10% expansion of the gold lattice. Then, it is relaxed to about 3% of the bulk value. These results mean that the gold particle is in a tensile strain state. It may be noted that such measurement was only possible on one particle, then we cannot conclude on the generality of this phenomenon. Some of us have previously observed for gold particles obtained by vacuum evaporation on an anatase powder, an accommodation at the interface, which also corresponded to a dilatation of the gold lattice [41].

3.4. Catalytic reaction of CO oxidation

The two series of catalysts (DP NaOH and DP Urea) were tested in the reaction of CO oxidation at 5 °C as a function of the pretreatment temperature of the catalysts under air (100, 150, 200, 300, and 400 °C), after drying at 100 °C under vacuum.

Table 3 reports the average gold particle size measured by TEM for the DP Urea and DP NaOH catalyst series and shows that the average gold particle size increases with the calcination temperature. It may be noted that for the unreduced samples, DP Urea samples calcined at 100 or 150 °C and DP NaOH samples calcined at 100 °C, gold is reduced by the electron beam during TEM observa-

Table 3
Average particle size and standard deviation for the DP Urea and DP NaOH catalysts before and after CO oxidation for 5 h (except for the data preceded by the sign * whose catalyst was exposed for 48 h) as a function of calcination temperature

Temperature (°C)	Particle size in DP Urea (nm)		Particle size in DP NaOH (nm)	
	Before CO oxidation	After CO oxidation	Before CO oxidation	After CO oxidation
100	1.1 (0.37)[a]	1.4 (0.32)	1.5 (0.33)	1.5 (0.36)
150	1.5 (0.39)	1.4 (0.38)	1.7 (0.39)	1.8 (0.36)
200	2.3 (0.49)	2.2 (0.56)	2.0 (0.40)	2.1 (0.41)
300	2.6 (0.61)	2.5 (0.55)	2.2 (0.58)	2.4 (0.64)
400	3.4 (0.99)	3.2 (0.73)	3.5 (0.89)	3.4 (0.92)
300*	2.1 (0.41)	2.3 (0.54)	2.0 (0.36)	2.2 (0.51)

[a] Standard deviation (nm).

tion, and particles appear after a few seconds of exposition.

Fig. 5 shows that the activity ($mol_{CO}\, mol_{Au}^{-1}\, s^{-1}$) is a function of the calcination temperature. The activity of both series of catalysts varies with the calcination temperature as follows: 200 > 300 > 400 > 150 °C. The DP NaOH catalyst calcined at 100 °C presents a very low activity during the first hours of reaction and then becomes inactive, whereas the DP Urea catalyst calcined at 100 °C is fully inactive.

Table 3 reports the average gold particle sizes measured after ≈ 5 h of CO oxidation reaction. In both DP Urea and DP NaOH catalyst series, there is no change in gold particle size during reaction. This is an indication that the initial deactivation of the catalysts observed in Fig. 5 is not due to the sintering of the gold particles. Moreover, two DP Urea and DP NaOH catalysts calcined at 300 °C were submitted to 48 h of reaction, but the gold particle size did not increase significantly either (Table 3). As a consequence, the hypothesis of deactivation due to an increase in particle size, as proposed by Valden et al. [42], is not confirmed by our results. It may be noted that several other causes of deactivation are proposed in the literature. Deactivation could be due to water adsorbed on the titania interfacial sites according to Bollinger and Vannice [43], to the carbon adsorption on the catalytic sites, according to Srinivas et al. [44], to the build up of impurities on the catalyst surface, as suggested by Schubert et al. [45] and Daté et al. [16]. Costello et al. [25] report that on Au/Al_2O_3, deactivation cannot be due to adsorbed CO or carbon deposit, and that the catalysts can be successfully regenerated with water.

4. Discussion

According to the XANES, EXAFS, and UV-visible absorption results, the reducibility of gold depends on the preparation method. It occurs at lower temperatures on DP NaOH than on DP Urea samples. Indeed, XANES and EXAFS showed that Au^{III} begins to reduce into Au^0 after calcination at 100 °C for the DP NaOH samples, and after calcination at 150 °C for the DP Urea samples (Figs. 2 and 3 and Tables 2 and 3). These results agree with those obtained by UV-visible spectroscopy (Fig. 1). The presence of the plasmon band at ∼ 550 nm, characteristic of metallic gold, also permits a rough evaluation of the percentage of metallic gold.

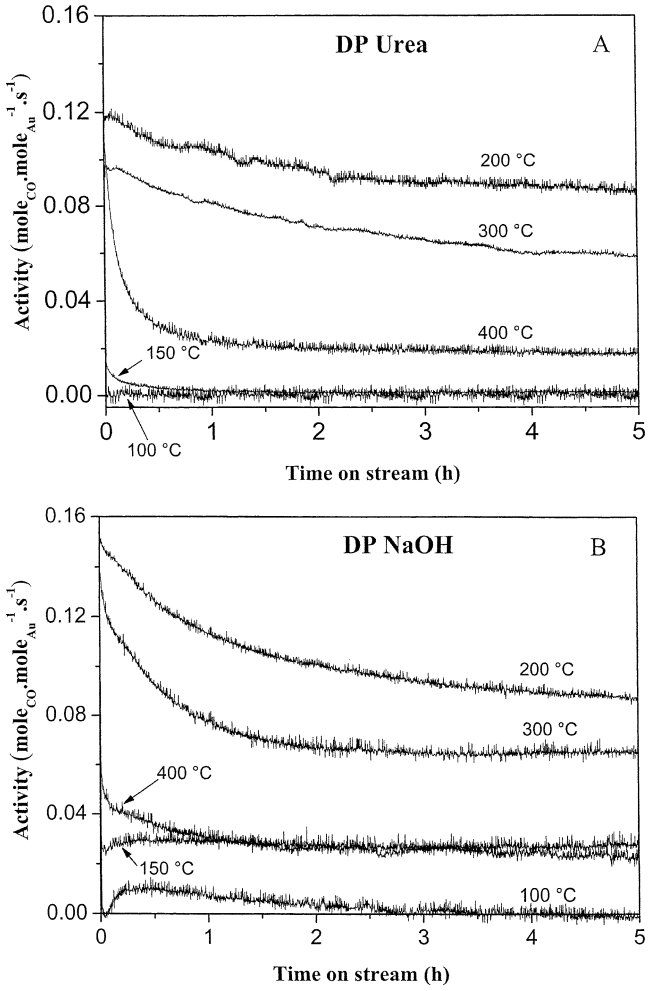

Fig. 5. Activity in CO oxidation of the DP Urea (A) and DP NaOH samples (B) versus the time on stream for various temperatures of calcination (a) 100, (b) 150, (c) 200, (d) 300, and (e) 400 °C.

The difference in reducibility may be due to the fact that the Au species formed during the process of gold deposition on TiO_2 is not the same for the two preparation methods (unpublished results). Indeed, the mechanism of deposition-precipitation with NaOH is different from that with urea. For the first method, the pH is fixed by the addition of NaOH, and all gold is not deposited whereas for the second one, the pH increases with time, due to urea decomposition, and all gold is deposited within the first hour [9]. It may be noted that gold remains in the oxidation state III during preparation by both methods.

The temperature at which gold is found fully reduced (200 °C) on DP Urea and DP NaOH catalysts is lower than that reported by Haruta and colleagues [15,16], for Au/TiO_2 prepared by DP NaOH. They found that a significant fraction

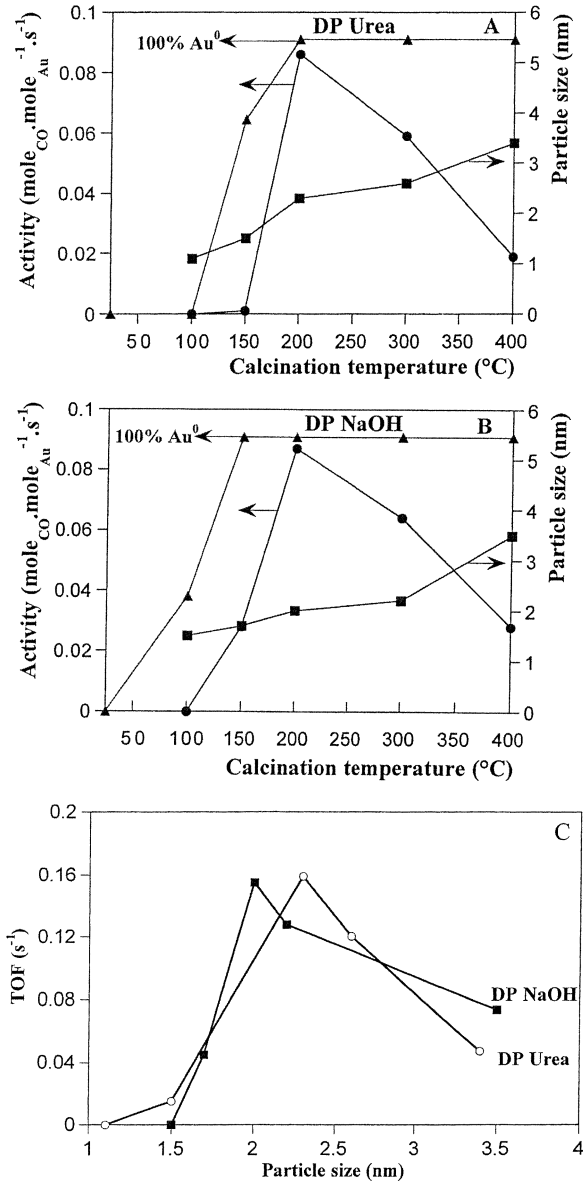

Fig. 6. Activity in CO oxidation (●), average particle size (■), and percentage of metallic gold (▲) of the DP Urea (A) and DP NaOH samples (B) versus the temperature of calcination; (C) TOF for CO oxidation as a function of the average particle size.

of gold was not metallic after calcination at 200 °C, and that only after calcination at 300 °C, all gold was reduced.

For DP NaOH and DP Urea catalysts, the onset of activity for CO oxidation appears after calcination at 100 and 150 °C, respectively (Figs. 5 and 6). These temperatures correspond to the appearance of metallic gold. At 200 °C, when all the gold is metallic in both catalysts, the maximum in activity is reached.

The nature of the active gold phase in Au/TiO_2 catalysts for CO oxidation is still controversial. In the specific case of Au/TiO_2, Park and Lee [18] concluded from XPS investigations that oxidized gold is more active than metallic gold. Guzman and Gates [26] concluded that in Au/MgO catalysts, both Au^I and Au^0 are the catalytically active species in CO oxidation. Costello et al. [25] suggested that for Au/Al_2O_3 catalysts, the active site would be an ensemble constituted by an hydroxyl group associated with an Au^I cation (Au^+–OH^-) linked to Au^0 particles.

On the contrary, other authors concluded from FTIR and XPS studies that metallic gold was the active species in Au/TiO_2 [2,31,32] or in $Au/Ti(OH)_4$ [34]. No Au^I species was observed by Haruta [5] in Au/TiO_2 catalysts. They proposed that the active gold species is Au^0, and that it is necessary for the adsorption of CO.

Our results rather support the second hypothesis since we found a clear correlation between the catalytic activity and the proportion of metallic gold in the catalysts for the two types of preparation methods investigated here. However, it cannot be excluded that a small fraction of the gold species would not be reduced, since oxidized species cannot be detected by TEM, or by XAS if the fraction corresponds to less than 10% of the Au present in the samples.

We have shown that the average gold particle size increased moderately with the calcination temperature (Figs. 6A and 6B). To take into account the increase of size, we have calculated the TOFs as described under Experimental, from the activity values obtained after 5 h of reaction (Fig. 6C). It may be noted that the TOF values of the samples pretreated at 100 °C (DP Urea and DP NaOH) and 150 °C (DP Urea) are not correct since the gold particles are not fully reduced at these temperature, but they become metallic under the electron beam of the microscope. The fact that the TOFs are very close for the two types of catalysts indicates that the method of preparation has no influence on the catalytic properties. This has been also observed in the case of selective hydrogenation reaction by some of us (submitted to J. Catal.). This is a remarkable feature because of the very different gold loadings in the two types of catalysts (∼ 3 wt% in DP NaOH and ∼ 8 wt% in DP Urea). This indirectly confirms that the gold dispersion is the same in the two types of catalysts, in agreement with the particle size measurements.

The decrease of activity for calcination temperatures higher than 200 °C (Figs. 5 and 6) obviously cannot be due to the evolution of the oxidation state of gold because it is already purely metallic. It can be related to the variation of the particle size which increases with the calcination temperature (Figs. 6A and 6B). However, between 200 and 300 °C, the size is almost constant, although the TOF drops by more than 30% (Fig. 6C). Moreover, in comparison with previous results of Haruta [2] and Goodman and colleagues [7], our maximum of activity occurs at a significantly smaller particle size (2 instead of 3–4 nm). The size effect and our variations of TOF are much less drastic than those reported by these two teams. The size effect observed by Goodman and colleagues [7] was explained by an evolution of the electronic structure of the gold clusters (grown on UHV on the (110) face of rutile). When the particle height is below a certain limit, a band gap opens,

and increases when the cluster height decreases. According to these authors, the maximum of activity results from the presence of 2 monolayer (ML) thick particles, and the activity significantly decreases for particles of 3 ML. This is not the case of our catalysts since after calcination at 200 °C, the gold particles are 5 to 7 ML thick, as observed by HRTEM (Fig. 4A); thus they certainly have the electronic structure of bulk gold [17]. Of course, we cannot rule out the fact that some small ($\leqslant$ 1 nm) and raft-shape particles, nonvisible in HRTEM, may not be present in our samples.

Rather than a pure size effect, we propose that the decrease of TOF is mainly due to an evolution of the particle morphology with the pretreatment temperature. We can see on the HRTEM micrographs (Fig. 4A) that the gold particles obtained after pretreatment at 200 °C do not exhibit well-developed facets. On the contrary, those obtained after pretreatment at 500 °C (Fig. 4B) are perfectly facetted with low index planes. Therefore, the proportion of low coordination sites is much lower after pretreatment at 500 °C (or at 300–400 °C) than at 200 °C. Therefore, the decrease in catalytic activity and TOF when the calcination temperature increases from 200 to 400 °C is attributed to the smoothing of the outer surface of the gold particles, i.e., to the decrease in the number of low coordinated sites. Since, CO can easily adsorb on gold particles and that O_2 adsorption is the rate-limiting step for this reaction, we propose that the changes in activity observed in this work (Fig. 6) are related to the changes in the proportion of the low coordination sites on which O_2 could be adsorbed. This interpretation is reinforced by recent calculations, which have shown that on low coordinated sites, the binding energy of oxygen increases, and its dissociation barrier decreases [17].

Another effect, which could also play a role on the catalytic activity of the gold particles, is the strain of the gold lattice. This has been recently suggested from the observation that gold clusters grown under UHV on anatase [41] showed a tensile strain up to 12%. Moreover, recent calculation by Xu and Mavrikakis [46] have shown that on a 10% tensile-stretched Au(111) surface, O_2 can dissociate with a barrier height of 1.37 eV whereas this is not possible on the unstretched surface. On a more open surface such as Au(211), the dissociation barrier is 0.63 eV only, with the same amount of strain, instead of 0.88 eV. Therefore, the best sites for dissociation of oxygen molecules are steps presenting a tensile strain. We have indeed shown on one gold particle obtained after pretreatment at 500 °C, and in epitaxy on the rutile TiO_2 support (Figs. 4B and 4C), that it presents a tensile strain, which is larger near the interface. Thus, the interface gold atoms could be even more active than the other surface atoms. However, this effect is probably of minor importance in the present work since only one particle was observed in epitaxy and only after treatment at a temperature higher than 300 °C. We believe that the activity of gold particles is related to the number of low coordinated surface atoms.

5. Conclusion

In summary, we have prepared Au/TiO_2 catalysts by two methods, deposition-precipitation with NaOH (DP NaOH) and deposition-precipitation with urea (DP Urea). The gold loadings are different, 3 and 8 wt%, respectively. The difference is due to the fact that all gold of the solution is deposited on TiO_2 in the case of DP Urea and not in the case of DP NaOH. From UV-visible absorption spectroscopy and XANES, it has been shown that by increasing the calcination temperature (100 to 300 °C), the gold species evolve from an oxidic state (Au^{III}) to a pure metallic one, which is reached at 200 °C for the two preparation methods. However, the reduction of gold starts at a lower temperature for the DP NaOH (100 °C) than for DP Urea catalysts (150 °C). The EXAFS results support these findings by the fact that for the samples calcined at a temperature below 200 °C, Au–O distances are observed whereas after calcination at 200 °C, only Au–Au distances are observed. TEM observations show that the size of the gold particles increases from 1.5 to 3.5 nm when the calcination temperature increases up to 400 °C. The catalytic activity for CO oxidation starts when metallic gold starts forming. It is maximum after a calcination temperature of 200 °C, for both types of preparation, when all the gold is metallic. At higher calcination temperature, the activity drops. The activities expressed per mole of Au and the TOF are the same for both types of catalysts, and evolve in the same way. The decrease of activity and TOF with the calcination temperature mainly arises from the decrease of the number of low coordinated sites on the surface of the gold particles due to a change of particle shape. Indeed, HRTEM has shown that after calcination at 200 °C, the gold particles present small facets with large rounded parts whereas after calcination at high temperatures, they are perfectly facetted with smooth and low index facets. The high activity on low coordinated gold atoms is in line with recent ab initio calculations.

Acknowledgments

Rodolfo Zanella is indebted to CONACYT (Mexico) and SFERE (France) for his Ph.D. grant, and to FESC, UNAM. We also thank the technical staff of LURE synchrotron facility (Orsay, France) and especially Dr Françoise Villain.

References

[1] B. Hammer, J.K. Norskov, Nature 376 (1995) 238.
[2] M. Haruta, Catal. Today 36 (1997) 153.
[3] M. Haruta, T. Kobayashi, H. Sano, N. Yamada, Chem. Lett. 2 (1987) 405.
[4] G.C. Bond, D.T. Thompson, Catal. Rev.-Sci. Eng. 41 (1999) 319.
[5] M. Haruta, Chem. Record 3 (2003) 75.
[6] G.R. Bamwenda, S. Tsubota, T. Nakamura, M. Haruta, Catal. Lett. 44 (1997) 83.
[7] M. Valden, X. Lai, D.W. Goodman, Science 281 (1998) 1647.

[8] S. Tsubota, D.A.H. Cunningham, Y. Bando, M. Haruta, Stud. Surf. Sci. Catal. 91 (1995) 227.
[9] R. Zanella, S. Giorgio, C.R. Henry, C. Louis, J. Phys. Chem. B 106 (2002) 7634.
[10] S. Tsubota, M. Haruta, T. Kobayashi, A. Ueda, Y. Nakahara, Stud. Surf. Sci. Catal. 72 (1991) 695.
[11] A.P. Kozlova, S. Sugiyama, A.I. Kozlov, K. Asakura, Y. Iwasawa, J. Catal. 176 (1998) 426.
[12] T. Akita, P. Lu, S. Ichikawa, K. Tanaka, M. Haruta, Surf. Interf. Anal. 31 (2001) 73.
[13] A. Wolf, F. Schüth, Appl. Catal. A 226 (2002) 1.
[14] M. Haruta, S. Tsubota, T. Kobayashi, H. Kageyama, M.J. Genet, B. Delmon, J. Catal. 144 (1993) 175.
[15] F. Boccuzzi, A. Chiorino, M. Manzoli, P. Lu, T. Akita, S. Ichikawa, M. Haruta, J. Catal. 202 (2001) 256.
[16] M. Daté, Y. Ichihashi, T. Yamashita, A. Chiorino, F. Boccuzzi, M. Haruta, Catal. Today 72 (2002) 89.
[17] M. Mavrikakis, P. Stoltze, J.K. Norskov, Catal. Lett. 64 (2000) 101.
[18] E.D. Park, J.S. Lee, J. Catal. 186 (1999) 1.
[19] W.E. Epling, G.B. Hoflund, J. Weaver, S. Tsubota, M. Haruta, J. Phys. Chem. 100 (1996) 9929.
[20] S.D. Gardner, G.B. Hoflund, M.R. Davidson, H.A. Laitinen, D.R. Schryer, B.T. Upchurch, Langmuir 7 (1991) 2140.
[21] A.M. Visco, A. Donato, C. Milone, S. Galvagno, Reac. Kinet. Catal. Lett. 61 (1997) 219.
[22] A.M. Visco, F. Neri, G. Neri, C. Milone, S. Galvagno, Phys. Chem. Chem. Phys. 1 (1999) 2869.
[23] S. Minicò, S. Scirè, C. Crisafulli, A.M. Visco, S. Galvagno, Catal. Lett. 47 (1997) 273.
[24] R.D. Waters, J.J. Weimer, J.E. Smith, Catal. Lett. 30 (1995) 181.
[25] C.K. Costello, M.C. Kung, H.-S. Oh, K.H. Kung, Appl. Catal. A 232 (2002) 159.
[26] J. Guzman, B.C. Gates, J. Phys. Chem. B 107 (2003) 2242.
[27] A. Sanchez, S. Abbet, U. Heiz, W.D. Schneider, H. Häkkinen, R.N. Barnett, U. Landman, J. Phys. Chem. A 103 (1999) 9573.
[28] D.M. Cox, R. Brickman, K. Creegan, A. Kaldor, Z. Phys. D 19 (1991) 353.
[29] B.E. Salisbury, W.T. Wallace, R.L. Whetten, Chem. Phys. 262 (2000) 131.
[30] W.T. Wallace, R.L. Whetten, J. Am. Chem. Soc. 124 (2002) 7499.
[31] M.A.P. Dekkers, M.J. Lippits, B.E. Nieuwenhuys, Catal. Lett. 56 (1998) 195.
[32] J.D. Grunwaldt, M. Maciejewski, O.S. Becker, P. Fabrizioli, A. Baiker, J. Catal. 186 (1999) 458.
[33] A.I. Kozlov, A.P. Kozlova, H. Liu, Y. Iwasawa, Appl. Catal. A 182 (1999) 9.
[34] H. Liu, A.I. Kozlov, A.P. Kozlova, T. Shido, K. Asakura, Y. Iwasawa, J. Catal. 185 (1999) 252.
[35] A. Michalowicz, in: EXAFS pour le MAC, Logiciels pour la Chimie, vol. 102, Soc. Fr. Chimie, Paris, 1991.
[36] B. Lengeler, P. Eisenberger, Phys. Rev. B 21 (1980) 4507.
[37] F. James, M. Ross, Comput. Phys. Commun. 10 (1975) 343.
[38] J.M. de Leon, J.J. Rehr, S.I. Zabinsky, R.C. Albers, Phys. Rev. B 44 (1991) 4146.
[39] J.J. Rehr, J.M. de Leon, S.I. Zabinsky, R.C. Albers, J. Am. Chem. Soc. 113 (1991) 5135.
[40] A. Zwijnenburg, A. Goossens, W.G. Sloof, M.W.J. Crajé, A.M. van der Kraan, L.J. de Jongh, M. Makkee, J.A. Moulijn, J. Phys. Chem. B 106 (2002) 9853.
[41] S. Giorgio, C.R. Henry, B. Pauwels, G.P. Tendeloo, Mater. Sci. Eng. A (2000).
[42] M. Valden, S. Pak, X. Lai, D.W. Goodman, Catal. Lett. 56 (1998) 7.
[43] M.A. Bollinger, M.A. Vannice, Appl. Catal. B 8 (1996) 417.
[44] G. Srinivas, J. Wright, C.S. Bai, R. Cook, Stud. Surf. Sci. Catal. 101 (1996) 427.
[45] M.M. Schubert, V. Plzak, J. Garche, R.J. Behm, Catal. Today 76 (2001) 143.
[46] Y. Xu, M. Mavrikakis, J. Phys. Chem. B 107 (2003) 9298.